ADNI Alzheimer's Disease Neuroimaging Initiative

Fully-Automated White Matter Hyperintensity Detection With Anatomical Prior Knowledge and Without FLAIRs

Christopher Schwarz, Evan Fletcher, Charles DeCarli, and Owen Carmichael
University of California, Davis

Contents

Page 1 Summary
Page 1 Introduction
Page 2 Data and Preprocessing
Page 2 Method
Page 4 Summary of Results
Page 4 References
Page 5 About The Authors

Summary

This method is designed for detection of cerebral white matter hyperintensities (WMH) based on run-time PD-, T1-, and T2- weighted structural magnetic resonance (MR) images of the brain along with labeled training examples. Its success is due to the learning of probabilistic models of WMH spatial distribution and neighborhood dependencies from ground-truth examples of FLAIR-based WMH detections. These models are combined with a probabilistic model of the PD, T1, and T2 intensities of WMHs in a Markov Random Field (MRF) framework that provides the machinery for inferring the positions of WMHs in novel test images. Prior work shows that standard off-the-shelf MRF training and inference methods provide robust results and that increasing the complexity of neighborhood dependency models does not necessarily help performance[1, 2]

Introduction

Because T1-weighted and double echo PD/T2-weighted acquisitions are nearly ubiquitous in large-scale imaging studies, this method focuses on WMH detection based solely on T1, T2, and PD input images. We do, however, use FLAIR for training data and the validation of automated methods (Fig. 1). WMHs are hyperintense on PD and T2, and hypointense on T1, but none of these modalities provide sufficient contrast between normal white matter (WM) and WMHs (Fig. 1). Therefore, we combine image intensity information with prior anatomical knowledge about where WMHs are known to occur in the brain and how they progress over time from one part of the brain to another. In particular, we employ a **spatial prior**– the prior probability of a WMH occurring at a given pixel, irrespective of imaging data– and a **contextual prior**– the conditional probability of a WMH occurring at a given pixel, given that WMHs have occurred at neighboring pixels. In elderly subjects, the spatial and contextual priors are highly structured and capture a characteristic spatial distribution of WMH occurrence and progression; specifically, WMHs in Alzheimer's disease and healthy aging tend to begin in periventricular zones and spread upward and outward (see Fig. 2 and Yoshita et al. [3]). The prior models that capture this progression are learned from FLAIR-based ground-truth WMH detections in a training phase and are combined with intensity information at run-time in an MRF framework to detect WMHs in novel sets of coregistered (PD, T1, T2) test image sets.

Figure 1. A representative axial slice from the input images used for detecting WMHs at run time (left) and ground-truth data used for training the WMH detection method and validating the results (right).

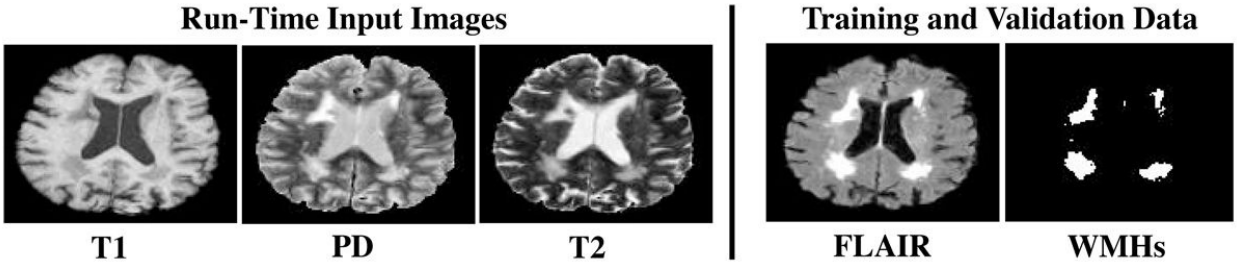

Figure 2. Left: ADC subjects were divided into quintiles based on total WMH volume; voxels that had WMHs in more than 5% of subjects in the quintile are shown in red. Note that WMHs appear to progress systematically upwards and outwards from periventricular zones. **Right:** The contextual prior captures the characteristic inferior-to-superior progression of WMHs in elderly subjects. Each pixel is colored according to the probability that it is WMH, given that the pixel below it, *vs.* above it, is WMH. *P*(*WMH*|*WMHBelow*) is moderate at most pixels because if a downward neighbor is WMH, the upward propagation of WMHs may have arrived there and stopped; or it may have continued upward to include the pixel in question. Meanwhile *P*(*WMH*|*WMHAbove*) is generally high because if the upward progression of WMHs has already reached a particular pixel, it is likely to have already passed through the pixels below it. The WMH detection method uses this known spatial progression of WMH to help determine which pixels are WMH, based on the absolute position of the pixel and the presence of neighboring WMHs.

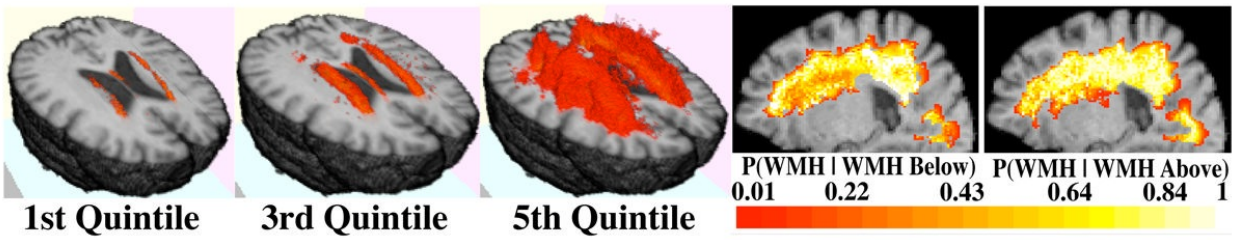

Data and Preprocessing

All scans were pre-processed through a standardized pipeline. T1, T2, PD, and FLAIR were rigidly coregistered using cross-correlation as a similarity measure and previously-presented optimization methods [4]. Nonbrain tissues were manually separated from the brain on all scans. A strongly-validated, semi-automated method was used to detect WMHs based solely on the FLAIR scans and human input [5]. The skull-stripped T1-weighted image was then nonlinearly aligned to a minimum deformation template (MDT) based on moving control points in a multi-scale grid and using cubic spline interpolation to move image pixels between the control points [6, 7].The warp is constrained such that no region is permitted to collapse entirely. The T1, T2, PD, FLAIR, and map of ground-truth FLAIR-based WMH pixels were then warped to the space of the MDT image using the nonlinear alignment.

Method

The details of this method are published[1] and the interested reader can refer to this publication for the specific theory on which it is based and the details of implementation. In brief, this method utilizes a Bayesian Markov-Random Field (MRF) approach to WMH detection established from a vector of three image intensities– PD, T1, and T2– associated with image pixel (Fig 3). Our goal is to determine a binary label for each image voxel that denotes either the presence or absence of a WMH at that voxel. This is accomplished utilizing the three image intensity vectors that maximize the posterior probability of the labels given the image intensity data. Within Bayes' theorem modified by MRF, the prior probability of a specific label depends both on the spatial prior– the prior probability that WMHs occur at given pixel as well as well as the contextual prior (i.e. the conditional probability of each voxel given the labels at neighbors of that voxel). The likelihood depends on the statistical distribution of the (PD, T1, T2) image intensities relative to the underlying labels.

Figure 3. The intensity distributions of WM and WMH intensities empirically follow "comet-like" patterns. WMH intensities and the fit distribution for them in one ADC subject is pictured in this graphic.

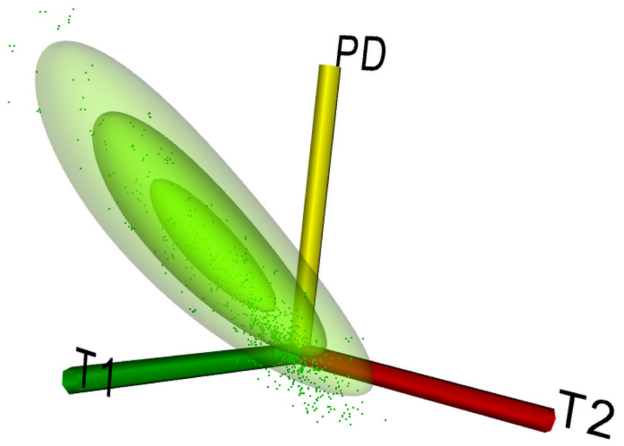

Training Set Size

One important property of any training-based classification method is the amount of training data it requires to give good results on test data. To test this property, we trained upon three different randomly selected subsets of the ADC dataset for each size: 10, 20, 40, 60, 80, and 100 subjects. We then ran the method to classify the dataset using these subsets as training data (Fig. 4). For this dataset our method performs better when using more training data up until about 60 images, after which there is little improvement.

Figure 4.
Plotted mean μ and $\mu \pm \sigma$ of ICC values between ground-truth WMH volume and WMH volume estimated by our method using differently-sized random subsets of the training set in cross validation. Note that these values are absolute, not percents, and are out of a maximum of 114 (training with all data). *Each of the size-10 ICC measures is without 1–2 test subjects for whom IPF did not converge.

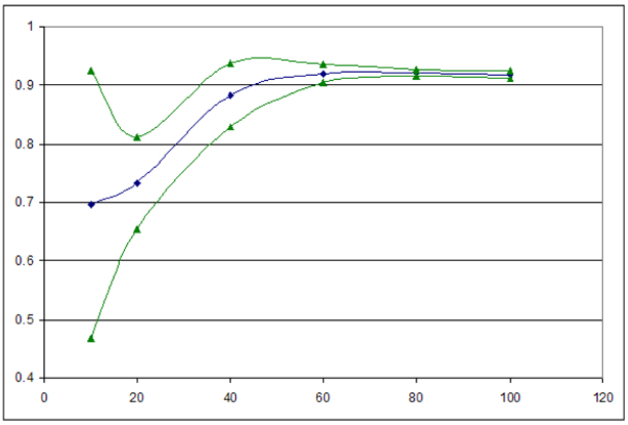

Training and Test Sets from Different Populations and Scanners
To test our method's performance using a completely different dataset from that upon which it was trained, we employed ground-truth WMH map data of 51 subjects from the Chicago Health and Aging Project (CHAP), a longitudinal Epidemiological study of individuals with risk factors for Alzheimer's disease. These images were preprocessed in the same fashion as the ADC data and used for training. We then tested (using 6-connected neighborhoods and standard training/inference) our dataset of 114 ADC subjects using this training data and obtained results with an ICC of 0.841, demonstrating our method's ability to perform reasonably when classifying images from a dataset from an entirely different MRI scanner, study type (epidemiological vs. clinic-based cohorts), and population.

Summary of Results
Our method performs robust WMH detection with no FLAIR when using at least 60 training images and standard MRF training/inference, including when the sources of training and testing data differ significantly. While our method performs strongly in these experiments, there exist several routes through which it can be improved in the future.

Dataset Information

This methods document applies to the following dataset(s) available from the ADNI repository:

Dataset Name	Date Submitted
UCD - WMH Volumes	15 December 2013

References

1. *Schwarz C, Fletcher E, DeCarli C, Carmichael O. Fully-automated white matter hyperintensity detection with anatomical prior knowledge and without flair. Inf Process Med Imaging. 2009;21:239-251*
2. *Schwarz CG, Fletcher E, Singh B, Liu A, Smith N, Decarli C, et al. Most edges in markov random fields for white matter hyperintensity segmentation are worthless. Conference proceedings : ... Annual International Conference of the IEEE Engineering in Medicine*

and Biology Society. IEEE Engineering in Medicine and Biology Society. Conference. 2012;2012:2684-2687

3. *Yoshita M, Fletcher E, Harvey D, Ortega M, Martinez O, Mungas DM, et al. Extent and distribution of white matter hyperintensities in normal aging, mci, and ad. Neurology. 2006;67:2192-2198*
4. *DeCarli C, Fletcher E, Ramey V, Harvey D, Jagust WJ. Anatomical mapping of white matter hyperintensities (wmh): Exploring the relationships between periventricular wmh, deep wmh, and total wmh burden. Stroke. 2005;36:50-55*
5. *Yoshita M, Fletcher E, DeCarli C. Current concepts of analysis of cerebral white matter hyperintensities on magnetic resonance imaging. Top Magn Reson Imaging. 2005;16:399-407*
6. *Kochunov P, Lancaster JL, Thompson P, Woods R, Mazziotta J, Hardies J, et al. Regional spatial normalization: Toward an optimal target. Journal of computer assisted tomography. 2001;25:805-816*
7. *Otte M. Elastic registration of fmri data using bezier-spline transformations. IEEE transactions on medical imaging. 2001;20:193-206*

About the Authors

This document was prepared by Christopher G. Schwarz[1], Evan Fletcher[2], Charles DeCarli[2], and Owen Carmichael[1,2]. A [1] denotes authors at the Computer Science Department, University of California, Davis, and a [2] denotes authors at the Neurology Department, University of California, Davis. For more information please contact Owen Carmichael at ocarmichael@ucdavis.edu.